

Structure-Based Design and Screen of Novel Inhibitors for Class II 3-Hydroxy-3-methylglutaryl Coenzyme A Reductase from *Streptococcus pneumoniae*

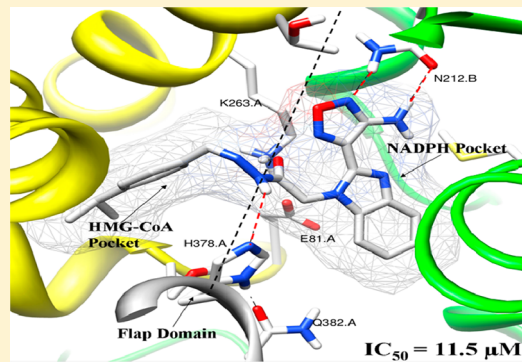
Ding Li,^{†,§} Jie Gui,^{†,§} Yongjian Li,[†] Lingling Feng,[†] Xinya Han,[†] Yao Sun,[†] Tinglin Sun,[†] Zhigang Chen,[†] Yi Cao,[†] Yang Zhang,[†] Li Zhou,[†] Xiaopeng Hu,[‡] Yanliang Ren,^{*,†} and Jian Wan^{*,†}

[†]Key Laboratory of Pesticide & Chemical Biology (CCNU), Ministry of Education, Department of Chemistry, Central China Normal University, Wuhan 430079, China

[‡]School of Pharmaceutical Science, Sun Yat-sen University, Guangzhou 510006, China

Supporting Information

ABSTRACT: 3-Hydroxy-3-methylglutaryl coenzyme A reductase (HMGR) is a primary target in the current clinical treatment of hypercholesterolemia with specific inhibitors of “statin” family. Statins are excellent inhibitors of the class I (human) enzyme but relatively poor inhibitors of the class II enzyme, which are well-known as a potential target to discover drugs fighting against the invasive diseases originated from *S. pneumoniae*. However, no significantly effective inhibitors of class II HMGR have been reported so far. In the present study, the reasonable three-dimensional (3D) structure of class II HMGR from *S. pneumoniae* (SP-HMGR-II) was built by Swissmodel. On the basis of the modeling 3D structure in “close” flap domain form, several novel potential hit compounds out of SPECs database were picked out by using structure-based screening strategy. Especially the compounds 4, 3, and 11 exhibit highly inhibitory activities, with IC₅₀ values of 11.5, 18.5, and 18.1 μM, respectively. Furthermore, the hit compounds were chosen as probe molecules, and their probable interactions with the corresponding individual residues have been examined by jointly using the molecular docking, site-directed mutagenesis, enzymatic assays, and fluorescence spectra, to provide an insight into a new special binding-model located between the HMG-CoA and NADPH pockets. The good agreement between theoretical and experimental results indicate that the modeling strategies and screening processes in the present study are very likely to be a promising way to search novel lead compounds with both structural diversity and high inhibitory activity against SP-HMGR-II in the future.



INTRODUCTION

3-Hydroxy-3-methylglutaryl coenzyme A reductase (HMGR, EC1.1.1.34) catalyzes the NAD(P)H-dependent reduction of HMGR to mevalonate, a four-electron oxidoreduction, which is the rate-limiting step in the endogenous synthesis of cholesterol and other isoprenoids. There are two distinct classes of HMGR, which appear to have arisen by divergent evolution from a common ancestor.¹ The class I HMGR (HMGR-I) enzymes present in eukaryotes and several archaea, and therefore, are critical target of statin drugs that severely attenuate cholesterol synthesis and lower blood cholesterol levels in human subjects² by competitive inhibition with respect to the substrate, HMG-CoA. The class II enzymes are utilized by prokaryotes and certain archaea and have been characterized including those from *P. mevalonii*, *Streptomyces sp.*, *S. aureus*, *S. pneumoniae*, and *A. fulgidus*^{3–8} and are well-known as a potential target for designing antibacterial drugs, especially those against the invasive diseases originated from *S. pneumoniae*.^{9–11} It is well-known that, *S. pneumoniae* was recognized as a major cause of pneumonia in the late 19th century, and is the subject of many

humoral immunity studies. Both enzymes share a common catalytic mechanism but exhibit significant difference in sensitivity to inhibition by statins.¹² The class II enzymes are considerably less sensitive to inhibition by statins drugs with *K_i* values in the range of millimolar, in contrast to the nanomolar values for the class I enzymes.^{7,12–14}

Great efforts have been made to design, synthesize, and develop the HMGR-I inhibitors,^{15–17} especially for the statins drugs with high inhibitory activities against class I enzyme.^{18,19} However, in addition to four natural products (Annonaceous acetogenins, ACGs) reported in our previous studies exhibit high inhibitory activity against HMGR-II,²⁰ no strongly effectively novel inhibitors of class II HMGR (HMGR-II) were reported hitherto. Since many of the ACGs exhibit outstanding cytotoxicity, the discovery of the novel potential inhibitors against HMGR-II is highly desirable. To meet the challenge of designing novel inhibitors with totally new

Received: March 27, 2012

Published: June 22, 2012



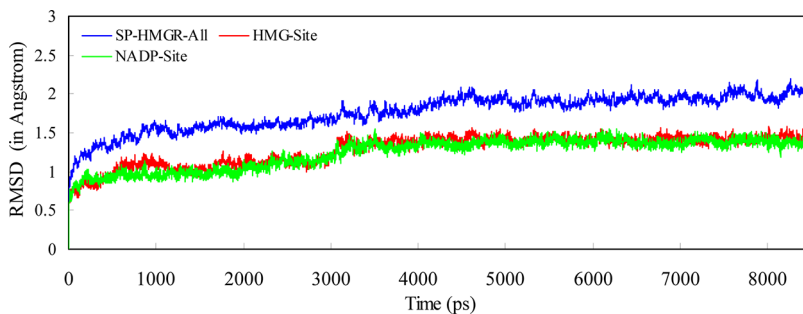


Figure 1. Plots of the MD simulation time vs root mean-square deviation (rmsd, in Å) for SP-HMGR-II modeling trajectories. The blue line represents the rmsd of the entire enzyme include the HMG-CoA and NADPH, the red line represents those of HMG-CoA active site, the green line represents those of NADPH active site.

molecular backbone and potency targeting the HMGR-II from *S. pneumoniae* (SP-HMGR-II), the knowledge of specifically critical binding site of ligands in the active site of target enzyme need to be clearly elucidated. To do this, an accurate three-dimensional (3D) structure of the target enzyme is a prerequisite. Previously, crystallographic work^{11,21,22} suggests that the active site of HMGR-II present at the homodimer interface between one monomer that binds the nicotinamide dinucleotide and a second monomer that bind HMG-CoA, the 3D dimeric structure of target enzyme is therefore required to construct the integral active pocket of SP-HMGR-II. To our knowledge, no effective crystal dimeric structure of SP-HMGR-II is resolved up to now, and the unique crystal monomeric structure of SP-HMGR-II was determined in our previous study.²³ Thus, in the present study, the homology modeling 3D dimeric structure of SP-HMGR-II was built by SWISSMODEL server.²⁴

The main purpose of this study is to explore a new pharmacophore models located between the HMG-CoA and NADPH pockets in SP-HMGR-II enzyme and to provide us the better information for designing the reasonable HMGR-II inhibitors in the future. To achieve this goal, a series of potential hit compounds were virtually filtered out from the SPECS database²⁵ by using the structure-based docking strategies, based upon the modeling 3D dimeric structure of SP-HMGR-II. The reliability of this method has been well documented in our previous publication.²⁶ The inhibitory assays *in vitro* for these compounds have been carried out, and then several hit compounds with new structural scaffold and high inhibitory activity were selected as probe molecules. Moreover, their probable interactions with the corresponding individual residues have been examined by jointly using the molecular docking, site-directed mutagenesis, enzymatic assays, and fluorescence spectra.

■ RESULTS AND DISCUSSION

Building of 3D Conformation of SP-HMGR-II and Overall Docking Strategy. Previously, Stauffacher et al.²² found that the active site of HMGR can be produced into the crystallographic structure with either the “open” or “close” flap domain form. In closed flap domain conformation, the last 50 residues of the C terminus (the flap domain) close on binding of the cofactor (NADPH) and positions the catalytic residues, whereas the flap domain is far from the active site and no direct interaction between the residues of flap domain and ligands (HMG-CoA or NADPH) can be observed in the “open” flap domain form. The recently crystallographic structure indicate that, the inhibitors of “statin” family are

indeed binding to active site of HMGR-I²⁷ and HMGR-II¹¹ in “open” flap form, because its bulky decalin ring interferes directly with closure of the flap domain. With this binding models, the inhibitors of “statin” family can exhibit significantly high inhibitory activity against HMGR-I, they however exhibit considerably less inhibitory activity against HMGR-II enzyme.¹¹ Furthermore, we have attempted to screen several compounds based upon the modeling structure of SP-HMGR-II with opened flap, but all of these compounds showed weak or no inhibitory activity. Both results demonstrate that it is actually difficult to discover the novel HMGR-II inhibitors based on the opened flap conformation, thereby the closed flap structure is likely to be an optimal target structure used in the design of potential and specific HMGR-II inhibitors. Fortunately, a X-ray crystallographic structure of HMGR-II from *P. mevalonii* (PDB ID: 1QAX) with “close” flap domain has been reported,²² which has, heretofore, established a solid molecular basis of the structure and mechanism for the development of novel potential inhibitors against SP-HMGR-II with “close” flap. Therefore, the crystallographic structure (1QAX) was selected as the template to build a 3D SP-HMGR-II model from the target sequence in this work.

In order to reduce steric clashes and further obtain the rational modeling 3D conformation of SP-HMGR-II, the molecular dynamic (MD) simulations have been further performed by using SANDER module of the AMBER8.0 package.²⁸ The rmsd for all atoms of the entire enzyme, the conserved residue within 6.5 Å from any given atom of HMG-CoA or NADPH were calculated, respectively, over the simulation time by using PTTRAJ module. The plots of the evolution of rmsd with simulation time were illustrated in Figure 1. The blue line represents the rmsd of entire enzyme between the simulated trajectories and the initial structure of whole enzyme. The red line represents the rmsd of conserved amino acid residue within 6.5 Å from any given residues of HMG-CoA, while the green line denotes the rmsd of the conserved amino acid residue within 6.5 Å from any given residues of NADPH. It is clear from Figure 1 that the conserved residues within 6.5 Å from HMG-CoA and NADPH achieved a dynamic convergence at around 4000 ps, respectively, while the whole enzyme system achieved a dynamics convergence at around 5000 ps. Although no dimeric crystallographic structure of SP-HMGR-II was reported up to now, the crystallographic monomeric structure (b chain) has been determined in our previous study.²³ Not surprising, the superposition between our modeling dimeric structure of SP-HMGR-II optimized by using MD simulation and crystallographic monomeric structure (b chain) shown that, for the b chain, the modeling conformation

is very similar to the crystal conformation, with a rmsd of 1.06 Å, as illustrated in Figure 2. The Ramachandran plot analyses²⁹

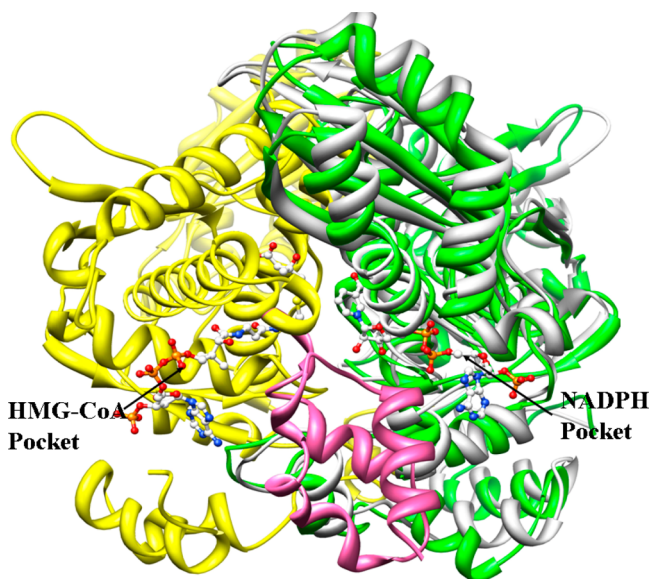


Figure 2. Schematics for the superposition of crystal monomer (B chain, white ribbon) and modeling dimeric structure of HMGR-II from *S. pneumoniae* by using molecular dynamic simulation (yellow and green ribbon). As for monomer (B chain), the modeling conformation is very similar to the crystal conformation with rmsd of 1.06 Å. The pink ribbon represents the flap domain.

confirmed the quality of the MD-based modeling 3D structure of SP-HMGR-II (Figure S1 of the Supporting Information), and the results show that 85.4% of the residues were distributed in the most favored regions, 12.5% in the additional allowed regions, 1.6% in the generously allowed regions, and only 0.6% in the disallowed regions, respectively. Hence, the 3D structure of the SP-HMGR-II enzyme was made available after carefully Molecular Dynamics simulation, and good quality 3D structure

of target enzyme was subsequently used in the Docking-based virtual screening investigation.

To test our docking protocol and validate the procedure, we also carried out docking experiments for the cofactor NADPH and substrate HMG-CoA. The initial geometric parameters of HMG-CoA backbone was extracted out of 1QAX, while the NADPH was built by SYBYL 7.3,³⁰ on which the hydrogen atoms were added, and subsequently submitted to a minimization by using the Tripos force field. The molecular docking results revealed that the binding modes of HMG-CoA and NADPH obtained by Surflex-Dock (the gray sticks in Figure 3) was almost identical to the crystallographic one (1QAX) (the light sea green lines in Figure 3), which gave us confidence in our protocol.

It is reported³¹ that the interface between NADPH pocket and HMG-CoA pocket is the catalytic region of HMGR, several residues in this region can participate in substrate catalysis. Especially, the active site histidine, glutamate, and aspartate are conserved in all known HMGR, and the changes in activity that accompany their mutagenesis support their proposed roles in catalysis.^{22,32–34} Apart from those known catalytic residues, our docking results (Figure 3) show that, at the NADPH pocket, the residue N212 can also form two remarkable hydrogen bonds with the NADPH nicotinamide. It is clear from the previous studies³⁵ that the nicotinamide group of NADPH acts as an electron donor and is a key factor in electron transfer during catalysis reaction of HMGR. Thus, these two hydrogen-bonds between residue N212 and nicotinamide are probably responsible for the proper orientation of nicotinamide, to ensure the high efficiency of electron transfer from cofactor NADPH to substrate HMG-CoA. In other words, if both hydrogen-bonds were broken by the N212 substitution, the orientation of nicotinamide is most likely to be changed, which in turn significantly affect the catalytic activity of NADPH. The mutant of N212 to Ala lacked detectable activity (Figure 4), which confirms this proposition. This is probably because the N212 is only residue binding with nicotinamide group of NADPH (Figure 3), and the mutant of N212 to Ala likely lead

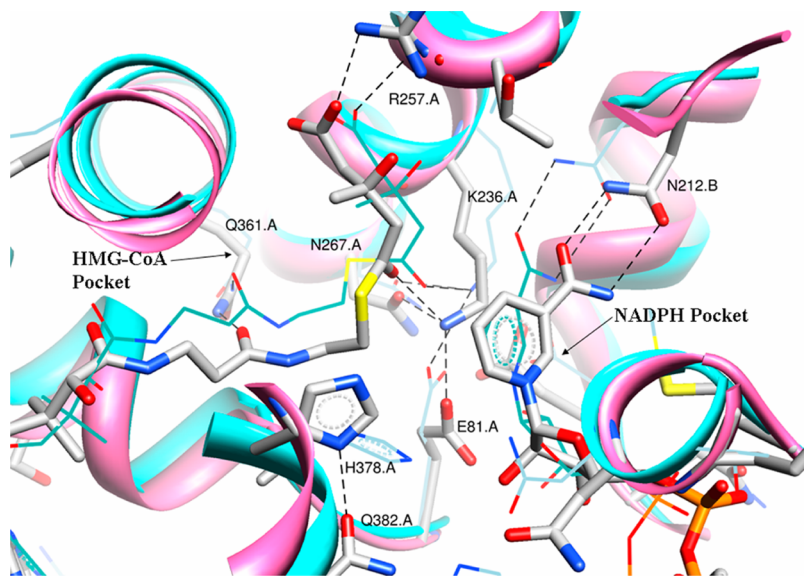


Figure 3. Superposition of template structure (1QAX, cyan ribbon) and modeling dimeric structure of SP-HMGR-II optimized by using MD simulation (hot pink ribbon), in which the gray sticks represent the modeling HMG-CoA and NADPH, the light sea green lines represent the crystal HMG-CoA and NADH.

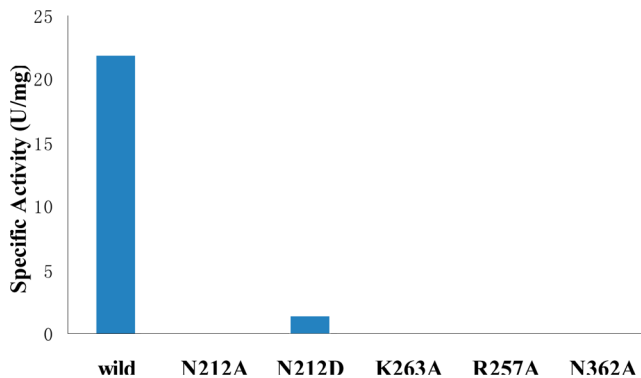


Figure 4. Schematic diagram of site-directed mutagenesis of SP-HMGR-II, together with the enzymatic specific activity of purified recombinant mutant protein.

to the complete disappearance of two hydrogen-bonds between nicotinamide group and residue N212, which ultimately result in the SP-HMGR-II exhibit no enzymatic activity. Furthermore, we also try to mutate the N212 to Asp (D), this substitution (N212D) can, in principle, form only one hydrogen-bond with NADPH nicotinamide group. As expected, the N212D substitution results in the catalytic constant ($k_{\text{cat}}[\text{HMG-CoA}] = 1.8 \times 10^3 \text{ S}^{-1}$ and $k_{\text{cat}}[\text{NADPH}] = 1.4 \times 10^3 \text{ S}^{-1}$) exhibit ~10-fold lower than the parental enzyme of SP-HMGR-II ($k_{\text{cat}}[\text{HMG-CoA}] = 4.8 \times 10^4 \text{ S}^{-1}$ and $k_{\text{cat}}[\text{NADPH}] = 1.5 \times 10^4 \text{ S}^{-1}$) (Table 1). Interestingly, as listed in Table 1, although the catalytic constant ($k_{\text{cat}}[\text{HMG-CoA}]$ and $k_{\text{cat}}[\text{NADPH}]$) of the N212D variant exhibited a significant drop, its enzyme kinetic parameter ($K_m[\text{HMG-CoA}] = 84.3 \mu\text{M}$ and $K_m[\text{NADPH}] = 58.5 \mu\text{M}$) exhibited a slight change from those of the parental enzyme ($K_m[\text{HMG-CoA}] = 75.7 \mu\text{M}$ and $K_m[\text{NADPH}] = 35.4 \mu\text{M}$), especially the value of $K_m[\text{NADPH}]$ of the N212D variant only exhibited a 2-fold increase compared to that of the parental enzyme. These experimental results show that N212 is a key residue in the catalytic function of NADPH and HMG-CoA, but not so important for the binding of NADPH. This is probably because the N212 is only the binding site for the nicotinamide group which can significantly affect the catalysis efficiency of NADPH. Conversely, a lot of interactions between NADPH and the closest other residues are evident (Figure 3), thus the interaction between NADPH and N212 only contributes a little to the binding of NADPH. The satisfactory theoretical explanation to the enzyme kinetic data of corresponding mutant protein implied that the binding mode of the ligand with the target protein obtained by Surflex-Dock was most likely valid and to some extent lent partial credit to the current modeling 3D structure of SP-HMGR-II as well.

Upon the basis of rationally modeling the 3D SP-HMGR-II structure, a set of virtual screen processes were performed. On the first step of 2D ligand-based searching, the criteria in terms of the Lipinski rules were employed to preselect all the molecules out of the SPECs database, after this processes

around 111 000 compounds were obtained for the following docking-based screening (as illustrated in Supporting Information Figure S2). All preselected compounds have been transformed from 2D to 3D by CONCORD module^{36,37} of SYBYL 7.3. A proper virtual screening cavity was generated in terms of the active site of the resultant 3D modeling structure of SP-HMGR-II. After the preceding Surflex-Dock processes, about 30 000 compounds were primitively selected out. Subsequently, in order to explore the specific inhibitors, those compounds (around 500 compounds) binding to not only the NADPH pocket but also the HMG-CoA pocket were selected from the compounds database screened in a previous step. Finally, we chose the residues N212, K236, and H378 as the important pharmacophore, those compounds (~35 compounds) directly interacted with these three residues were picked out from the compounds database obtained in last step. The reason why we chose these three residues as key pharmacophore is that, their crucial roles in the catalytic reaction of HMGR have been evident. It is clear from the previous study²² that, the K236 is at the center of a hydrogen bond network and can form several hydrogen bonds with the surrounding catalytic residues, and H378 is proximal to the sulfur atom of HMG-CoA, as would be expected for its proposed role in protonating the leaving CoAS⁻ anion.²² In addition, the N212 has also proved in the present study to be an essential residue, which can significantly affect the catalytic activity of target enzyme. Upon the basis of these screening strategy, several hit compounds with high inhibitory activity (IC_{50}) were ultimately screened, the groups of hit compounds located at NADPH pocket is colored blue, together with the corresponding inhibitory activities (IC_{50}) values, as listed in Tables 2 and 3.

Identification of the Binding Models of Hit Compounds. In Tables 2 and 3, the compound 4 show most highly inhibitory activities against SP-HMGR-II, with IC_{50} value of $11.5 \mu\text{M}$. We have therefore focused our investigations on this compound as a probe molecule, to further insight into the new pharmacophore models for SP-HMGR-II. In order to take into account the different structure, the compound 10 was also partially taken as another probe. The predicted binding modes of both probe molecules by molecular docking were illustrated in Figure 5.

On the NADPH pocket side, the nitro atom on oxadiazole ring and the amine connected to oxadiazole can form two remarkable hydrogen-bonds with the residue N212, which therefore likely contribute to the binding of hit compounds. In line with our docking prediction, the IC_{50} values (Table 1) of compounds 4 ($36.2 \mu\text{M}$) and 10 ($82.8 \mu\text{M}$) against the N212D variant are about 3-fold higher than parental enzyme (11.5 and $28.3 \mu\text{M}$), respectively. These experimental results clearly reveal that the mutant of N212 to Asp can remarkably affect the inhibitory activities of the hit compounds. Furthermore, according to the data in Table 4, the K_b values obtained from fluorescence quenching of compound 4 binding to N212D (5.1

Table 1. Kinetic Parameters of N212D Variants and Parental SP-HMGR-II Enzyme, as Well as the Inhibitory Activities (IC_{50}) of Compounds 4 and 10 against the Corresponding Target Protein

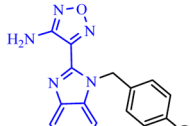
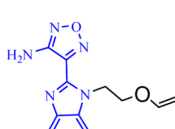
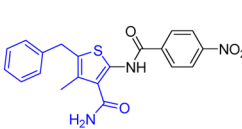
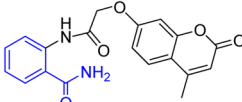
| | $K_m[\text{HMG-CoA}] (\mu\text{M})$ | $K_{\text{cat}}[\text{HMG-CoA}] (\text{S}^{-1})$ | $K_m[\text{NADPH}] (\mu\text{M})$ | $K_{\text{cat}}[\text{NADPH}] (\text{S}^{-1})$ | $\text{IC}_{50} (\mu\text{M})$ | |
|-------|-------------------------------------|--|-----------------------------------|--|--------------------------------|----------------|
| | | | | | 4 | 10 |
| N212D | 84.3 ± 4.5 | 1.8×10^3 | 58.5 ± 1.3 | 1.4×10^3 | 36.2 ± 2.3 | 82.8 ± 3.1 |
| wild | 75.7 ± 5.9 | 4.8×10^4 | 35.4 ± 2.4 | 1.5×10^4 | 11.5 ± 0.3 | 28.3 ± 1.2 |

Table 2. Molecular Structural Formulas of Hit Compounds and Corresponding Inhibitory Activities (IC_{50})

| Entry | R' | IC ₅₀ /μM | Entry | R | IC ₅₀ /μM |
|----------|----|----------------------|-----------|---|----------------------|
| 1 | | 57.3±3.1 | 5 | | 95.4±3.2 |
| 2 | | 39.2±2.3 | 6 | | 69.7±1.5 |
| 3 | | 18.5±1.8 | 7 | | 61.5±5.8 |
| 4 | | 11.5±0.4 | 8 | | 31.2±0.9 |
| | | | 9 | | 28.9±1.2 |
| | | | 10 | | 28.3±1.2 |
| | | | 11 | | 18.1±1.7 |

$\times 10^4 \text{ M}^{-1}$) and N212A ($6.1 \times 10^4 \text{ M}^{-1}$) variants are about 3-fold drop than the parental SP-HMGR-II ($14.43 \times 10^4 \text{ M}^{-1}$), it is consistent with the result obtained from the enzymatic assay of N212D variant. Combined with the enzymatic activities data

Table 3. Molecular Structural Formulas of Hit Compounds Together with Their Inhibitory Activities (IC_{50})

| Entry | Structure | IC ₅₀ (μ M) |
|-------|---|-----------------------------|
| 12 |  | 61.5±1.3 |
| 13 |  | 69.9±2.0 |
| 14 |  | 72.6±5.5 |
| 15 |  | 32.0±1.0 |

and the K_b values of N212D variant, we can conclude that the residue N212 is indeed important for the hit compounds binding and activity and the hydrogen bonds between the residue N212 and hit compounds likely exist.

At the catalytic region of active site of SP-HMGR-II, our docking results show that the acetamide of compounds **4** and **10** can form hydrogen bonds with the residues H378 and K263 (Figures 5A and 5B). However, it is impossible to recognize the theoretical predicted binding model directly through the enzymatic assay of H378A and K263A variants, since both variants exhibit too less enzymatic activity to continue the enzymatic assays studies (Figure 4). To further validate interaction between the hit compounds and these residues (H378 and K263), the binding constant (K_b) values of the corresponding variants have also been investigated by the fluorescence quenching experiment. The K_b value of the H378A variant is $3.4 \times 10^4 \text{ M}^{-1}$, respectively, which is at least 5-fold lower than the K_b value of $14.41 \times 10^4 \text{ M}^{-1}$ obtained for parental SP-HMGR-II. Especially, the K_b value of the K263A variant is $0.95 \times 10^4 \text{ M}^{-1}$, which exhibits a significant drop (around 15-fold) compared to those of the parental enzyme. It is clear from these data that the direct interactions (hydrogen bonds) of compound **4** with the residues H378 and K263 are evident, which contribute to the K_b change from H378A and K263A variants to the parental enzyme. It is suggested from previous study⁶ that, when the flap domain of HMGR is closed, the direct interactions between the flap domain and the ligands are apparent; conversely, the flap domain will be far from the ligands when the flap domain of HMGR is opened. Here, residue H378 is located in the flap domain, and the remarkable change of the K_b value of the H378A variant implied that the direct interaction between H378 and the hit compounds is exhibited. All theoretical and experimental results discussed above together suggested that the current set of hit compounds including **4** and **10** bind to a joint region between the HMG-CoA pocket and the NADPH pocket in the active site of SP-HMGR-II with the “close” flap domain, which is different from the binding mode (illustrated in Figure 6) of our previously reported ACGs,²⁰ a set of natural products with a long chain, exhibiting similar inhibitory activity against HMGR-II.

At the HMG-CoA pocket, the R-group connected to the acetamide of compounds **4** and **10** access to this region (Figure 5). Importantly, the R-group of all hit compounds screened in the present study possess the hydrophobic group (Tables 2 and 3), which imply the R-group region in this pocket is hydrophobic favorable as described previously.¹¹ Furthermore, the inhibitory activities of the hit compounds were remarkable affected by the substituent on phenyl ring, generally, the compounds with smaller substituent exhibit higher inhibitor activity. For instance, the inhibition activities of compounds **4** and **11** are ~5-fold higher than those of compounds **1** and **5** (Table 2). This result suggests that the bulky R-group fail to effectively situate into the HMG-CoA pocket, due to the steric hindrance effect.

■ CONCLUSION

In the present study, the reasonable three-dimensional structure of SP-HMGR-II was built by SWISSMODEL server. On the basis of the modeling the 3D conformation, a series of novel potential hit compounds with structural diversity were picked out by using structure-based screening strategy. Among these compounds, the compounds 4, 3, and 11 exhibit most highly inhibitory activities, with IC₅₀ values of 11.5, 18.5, and 18.1 μ M,

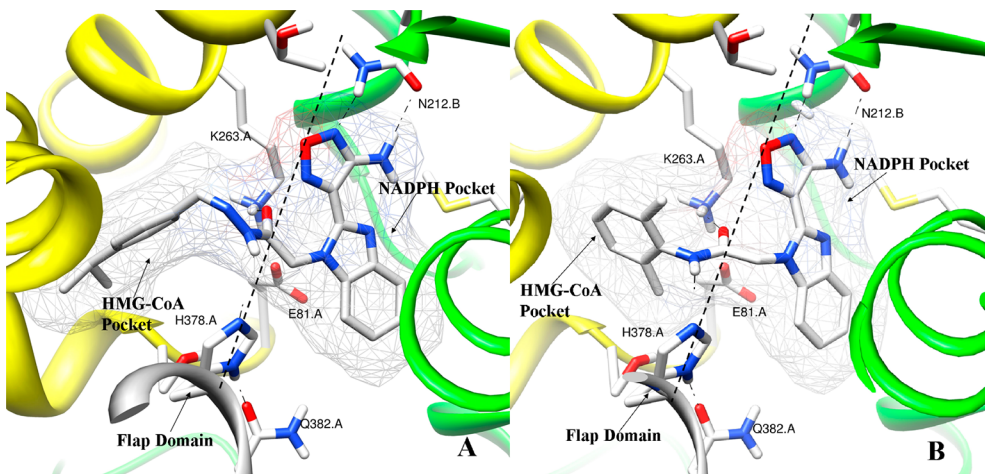


Figure 5. Optimal binding models of compounds 4 (A) and 10 (B) and into the active site of SP-HMGR-II docked by SURFLEX module. The target SP-HMGR-II enzyme is shown as a ribbon, in which the A chain is represented by a yellow ribbon and the B chain is represented by a green ribbon, while the gray ribbon denotes the flap domain; the hit compound and some key residues are shown in stick representation; and the hydrogen bonds are shown in dashed lines (black).

Table 4. Binding Constants (K_b) Determined by Fluorescence Quenching for Compound 4 Binding to the Parental SP-HMGR-II and Its Variants

| | $K_b (\times 10^4 \text{ M}^{-1})$ | n |
|-------|------------------------------------|------|
| WT | 14.43 | 1.12 |
| H378A | 3.40 | 0.99 |
| K263A | 0.95 | 0.91 |
| N212A | 6.10 | 1.05 |
| N212D | 5.10 | 1.02 |

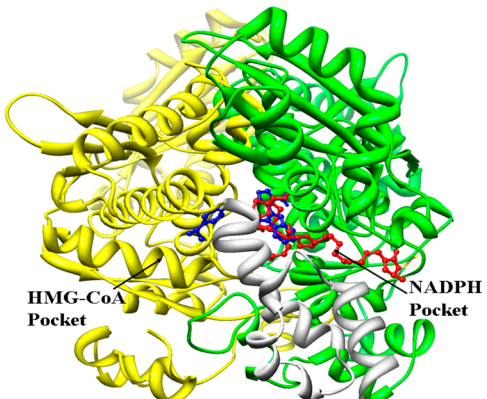


Figure 6. Optimal binding models of squamostatin A (red), one of ACGs, and compound 4 (blue) into the active site of SP-HMGR-II. The target SP-HMGR-II enzyme is shown in ribbon, in which the A chain is represented by yellow ribbon, B chain is represented by green ribbon, while the gray ribbon denotes the flap domain; small molecules are shown in ball and stick. Molecular docking studies predicted that compound 4 targeted toward a joint region between the HMG-CoA pocket and NADPH pocket, whereas squamostatin A was located in the whole NADPH pocket in SP-HMGR-II.

respectively. Taking the hit compounds as the probe molecules, the specifically new pharmacophore models of SP-HMGR-II were further investigated by jointly using the molecular docking, site-directed mutagenesis, and fluorescence spectroscopy experiments. An important new finding in this study is that the hit compounds can locate the joint region between the HMG-CoA and NADPH pockets in the active site of the target

enzyme. Furthermore, our results not only demonstrate that the residues N212, K263, and H378 are essential pharmacophores to the binding of the hit compounds in the present study but also suggest the current set of compounds are likely binding to the SP-HMGR-II in closed flap domain form, in contrast, the other known HMGR inhibitors are mainly binding to target enzyme in “open” flap form. The present theoretical and experimental results together provide new insights for the discovery of novel inhibitors directed against HMGR-II of pathogenic microorganism.

EXPERIMENTAL SECTION

Homology Modeling. On the basis of the sequence alignment, an accurate 3D structure of SP-HMGR-II was built by using the SWISSMODEL server (Automated Comparative Protein Modeling Server, Version 3.5, Glaxo Wellcome Experiment Research, Geneva, Switzerland).²⁴ The X-ray crystallographic structural information of HMGR-II from *P. mevalonii* (PDB ID: 1QAX) was selected as a template, the amino acid sequences of the SP-HMGR-II (sequence ID: AAG02454) were downloaded from NCBI, which has 40% sequence identity with the target enzyme, and the sequence alignment present in Figure S3 of the Supporting Information was used. All hydrogen atoms were subsequently added to the unoccupied valence of heavy atoms of modeling SP-HMGR-II at the neutral state by using the BIOPOLYMER module of the SYBYL 7.3 program package.³⁰

Molecular Dynamics Simulation. To reduce steric clashes and obtain reasonable modeling and 3D conformation of complex HMGR/HMG-CoA/NADPH from *S. pneumoniae*, a molecular dynamic (MD) study was also further performed by using SANDER module of AMBER8.0 package.²⁸ The leaprc.ff99 force field parameters were loaded for the enzyme system, and a set of default parameters provided by the AMBER8.0 was adopted for the cofactor NADPH. The whole system was first neutralized by adding Na⁺ cation and then solvated into an octahedral box of TIP3P water molecules,³⁸ which extended at least 10 Å from any given atom of enzyme system of interest. In addition, the following equilibration protocol was employed before starting the production-run phase. First, all water molecules of the TIP3P box were

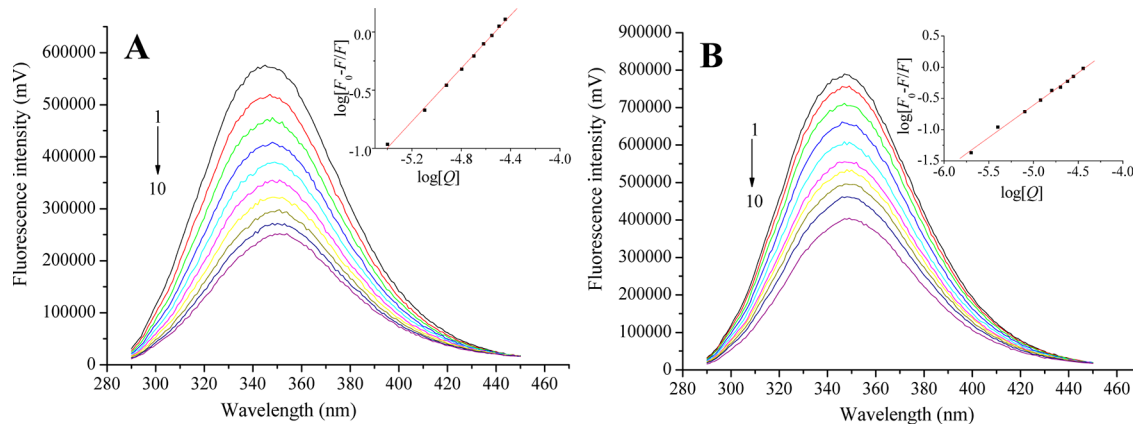


Figure 7. Fluorescence emission spectra of K263A variant (A) and parental SP-HMGR-II (B) titrated with compound 4, which was added to enzyme in 1.0 mL of 20 mM KH₂PO₄ (pH 6.5), and the concentrations of compound 4 are varying from 0 to 36 μM: (inset) plots of $\log[(F_0 - F)/F]$ versus $\log[Q]$.

minimized 2000 steps by steepest descent and 2000 steps by conjugate gradient, respectively, while holding the enzyme system frozen. Then whole system (enzyme plus water box) was minimized 4000 steps by using amber force field with releasing the whole system. Finally, the whole system was slowly heated from 0 to 300 K over 100 ps before MD simulation. Trajectories were recorded every 1 ps during the entire MD simulation process. A modeling averaged conformation was derived from the trajectories of the last converged 1000 ps and subjected to a subsequent minimization using Tripos force field of SYBYL7.3 with a rms gradient of 0.05 kcal/(mol·Å) to generate the final theoretically predictive 3D modeling conformation of SP-HMGR-II for subsequent virtual screening.

Docking-Based Virtual Screening. In order to explore the interaction mechanism and illustrate the accurate binding model for the active site of SP-HMGR-II with its ligands, molecular docking analysis was carried out by using SURFLEX module of SYBYL based on the target structure optimized by Molecular Dynamics methods. An “automatic” protocol was generated, and dockings were carried out using 20 initial conformations for each ligand; the Surflex-Dock scoring function³⁹ was used in these docking process. The active site was defined as follows: the modeling structure of SP-HMGR-II and the template protein (1QAX) were superposed first, and then, the NADH and HMG-CoA in crystal structure were merged into the corresponding site of the SP-HMGR-II modeling structure. All atoms located within the range of 6.5 Å from any atom of the HMG-CoA and NADH in the modeling protein were selected into the active site, the residue was included into the active site if at least one of its atoms was picked out.

By using the similar docking process, the structure-based virtual screening out of SPECS database was performed. The virtual screening strategy adopted in the present study also principally consisted of one step of 2D ligand-based searching in terms of Lipinski rules and two steps of 3D receptor–ligand binding mode-based molecular docking evaluations for the hit compounds out of SPECS database. On the first step of 2D ligand-based searching, the criteria in terms of the Lipinski rules (≤ 5 H-bond donors (no. of OH and NH groups), ≤ 10 H-bond acceptors (no. of O or N atoms), MW ≤ 500 Da, M log P ≤ 5) was employed to preselect all the molecules out of the SPECS database. Other default parameters were adopted in SURFLEX

docking and virtual screening. All calculations were performed on a CCNUGrid-based computational environment (CCNU-Grid Web site <http://202.114.32.71:8090/ccnu/chem/platform.xml>).

Bioaffinity Testing and Site-Directed Mutagenesis of SP-HMGR-II. To evaluate the inhibitory activity of hit compounds screened in the present study, the half maximal inhibitory concentration (IC₅₀) values of hit compounds were determined at the SP-HMGR-II recombinant protein level. The clone, expression, and purification of SP-HMGR-II recombinant protein, as well as a build-up of bioaffinity testing system in vitro were carried out as previously reported.²⁰ Before the enzyme was added, increasing concentration of each compounds were incubated for 5 min in a standard reaction mixture containing 50 mM NaCl, 1 mM EDTA, 25 mM KH₂PO₄, 5 mM DTT, 0.25 mM NADPH, and 100 μM HMG-CoA. The IC₅₀ were determined by nonlinear least-squares fitting of the data using the logistic kinetic equations from ORIGIN 7.0 software (Supporting Information Figure S4).

Mutations were accomplished by the introduction of specific base changes into a double-stranded DNA plastid. All highly effective site-directed mutagenesis were performed using KOD-Plus Mutagenesis kit (Toyobo, Osaka, Japan) according to the manufacturer’s protocol. The wild-type pET28a-SP-HNMR plasmid DNA template and mutagenic primers were denatured, annealed, and polymerized in a final volume of 50 μL for 25 cycles (94 °C for 20 s, 56 °C for 1 min, and 68 °C for 10 min). Dpn I restriction enzyme (Fermentas, China) was then used to digest parental methylated and hemimethylated DNA. The plasmids with mutations were transformed into *Escherichia coli* (*E. coli*) strain BL21 (DE3) cells and sequence analysis were performed for validations. Expression and purification of mutant enzymes were similar to those of wild-type SP-HMGR-II. On the basis of SDS-PAGE, all purified wild and mutant enzymes exhibit identical mobilities and purity greater than 95%.

Fluorescence Quenching Assay. Fluorescence measurements were performed at 37 °C with the Fluoro Max-P spectrophotofluorimeter, the excitation wavelength was 280 nm, and the emission spectrum was recorded in the 290–450 nm range in 1 mL quartz cuvettes. The concentration of parental SP-HMGR-II or variants of SP-HMGR-II with the H378A, N212A, N212D, and K263A substitutions was 0.2 mg/mL in 20 mM KH₂PO₄ buffer (pH 6.5). The excitation and emission

monochromator slit width were 3 nm. The ORIGIN software was used for the present data processing.

To further explore the detailed interactions of hit compounds with the variants and parental SP-HMGR-II, the fluorescence quenching technique was employed to measure the binding constants (K_b) for the representative compound 4. The K_b value of compound 4 was calculated using eq 1,^{40,41}

$$\log \frac{(F_0 - F)}{F} = \log K_b + n \log [Q] \quad (1)$$

F_0 is the initial fluorescence intensity of protein solution without the compound 4, F is the fluorescence intensities of protein solutions measured after the compound 4 was added, and $[Q]$ is the quenching concentration. We now show that, upon addition of compound 4 (Figure 7), the intrinsic fluorescence of parental SP-HMGR-II was diminished. An emission maximum at 350 nm is apparent, which very likely corresponds to the tryptophan residue. A plot of $\log[(F_0 - F)/F]$ versus $\log[Q]$ gives a straight line using least-squares analysis whose slope was equal to n (binding affinity), and the intercept on the Y axis was equal to $\log K_b$ (Figure 7).⁴² Upon the basis of the eq 1, the values of K_b and n for compound 4 against variants and parental SP-HMGR-II were therefore listed in Table 4. Importantly, both the variant and parental SP-HMGR-II exhibit similar binding affinity n (0.87–1.12) with compound 4, which suggest our hit compounds have one binding site within the target enzyme.

■ ASSOCIATED CONTENT

S Supporting Information

Figures S1–S4 show the schematic for the quality of the modeling, virtual screening protocol, sequence alignments on template and HMGR-II-SP target enzyme, and inhibition assay (IC_{50}). This information is available free of charge via the Internet at <http://pubs.acs.org>

■ AUTHOR INFORMATION

Corresponding Author

*Phone: +86-27-67862022. Fax: +86-27-67862022. E-mail: renyl@mail.ccnu.edu.cn (Y.R.); jianwan@mail.ccnu.edu.cn (J.W.).

Author Contributions

§These authors contributed equally to this study.

Notes

The authors declare no competing financial interest.

■ ACKNOWLEDGMENTS

This work was supported by the National Basic Research Program of China (973 Program, No. 2010CB126100), the Natural Science Foundation of China (Nos. 20873049, 20872044, 30900054, 21072073 and 21172089), Natural Science Foundation of Hubei Province (No. 2010CDB01202), the Program for Academic Leader in Wuhan Municipality (No. 201150530150), the self-determined research funds of CCNU from the colleges' basic research and operation of MOE (Nos. CCNU09A01010, CCNU10C01002, and CCNU10A02006), and the research was also supported in part by the PCSIRT (No. IRT0953).

■ ABBREVIATIONS USED

HMGR = 3-hydroxy-3-methylglutaryl coenzyme A reductase

HMGR-I = class I 3-hydroxy-3-methylglutaryl coenzyme A reductase

SP-HMGR-I = class I 3-hydroxy-3-methylglutaryl coenzyme A reductase from *Streptococcus pneumoniae*

HMGR-II = class II 3-hydroxy-3-methylglutaryl coenzyme A reductase

SP-HMGR-II = class II 3-hydroxy-3-methylglutaryl coenzyme A reductase from *Streptococcus pneumoniae*

LOV = lovastatin

■ REFERENCES

- (1) Bochar, D. A.; Stauffacher, C. V.; Rodwell, V. W. Sequence Comparisons Reveal Two Classes of 3-Hydroxy-3-methylglutaryl Coenzyme A Reductase. *Mol. Genet. Metab.* **1999**, *66*, 122–127.
- (2) Barnes, N. C. Drugs acting against leukotriene pathways current clinical knowledge. *Pharmacol. Res.* **1995**, *31*, 9–9.
- (3) Jordan-Starck, T. C.; Rodwell, V. W. Pseudomonas mevalonii 3-hydroxy-3-methylglutaryl-CoA reductase. Characterization and chemical modification. *J. Biol. Chem.* **1989**, *264*, 17913–17918.
- (4) Friesen, J. A.; Rodwell, V. W. The 3-hydroxy-3-methylglutaryl coenzyme-A (HMG-CoA) reductases. *Genome Biol.* **2004**, *5*, 248.1–248.6.
- (5) Beach, M. J.; Rodwell, V. W. Cloning, sequencing, and overexpression of *mvaA*, which encodes *Pseudomonas mevalonii* 3-hydroxy-3-methylglutaryl coenzyme A reductase. *J. Bacteriol.* **1989**, *171*, 2994–3001.
- (6) Takahashi, S.; Kuzuyama, T.; Seto, H. Purification, Characterization, and Cloning of a Eubacterial 3-Hydroxy-3-Methylglutaryl Coenzyme A Reductase, a Key Enzyme Involved in Biosynthesis of Terpenoids. *J. Bacteriol.* **1999**, *181*, 1256–1263.
- (7) Wilding, E. I.; Kim, D.-Y.; Bryant, A. P.; Gwynn, M. N.; Lunsford, R. D.; McDevitt, D.; Myers, J. E., Jr.; Rosenberg, M.; Sylvester, D.; Stauffacher, C. V.; Rodwell, V. W. Essentiality, Expression, and Characterization of the Class II 3-Hydroxy-3-Methylglutaryl Coenzyme A Reductase of *Staphylococcus aureus*. *J. Bacteriol.* **2000**, *182*, 5147–5152.
- (8) Kim, D. Y.; Ryu, S. Y.; Lim, J. E.; Lee, Y. S.; Ro, J. Y. Anti-inflammatory mechanism of simvastatin in mouse allergic asthma model. *Eur. J. Pharmacol.* **2007**, *557*, 76–86.
- (9) Wilding, E. I.; Brown, J. R.; Bryant, A. P.; Chalker, A. F.; Holmes, D. J.; Ingraham, K. A.; Iordanescu, S.; So, C. Y.; Rosenberg, M.; Gwynn, M. N. Identification, Evolution, and Essentiality of the Mevalonate Pathway for Isopentenyl Diphosphate Biosynthesis in Gram-Positive Cocci. *J. Bacteriol.* **2000**, *182*, 4319–4327.
- (10) Popják, G.; Boehm, G.; Parker, T. S.; Edmond, J.; Edwards, P. A.; Fogelman, A. M. Determination of mevalonate in blood plasma in man and rat. Mevalonate "tolerance" tests in man. *J. Lipid. Res.* **1979**, *20*, 716–728.
- (11) Tabernero, L.; Rodwell, V. W.; Stauffacher, C. V. Crystal Structure of a Statin Bound to a Class II Hydroxymethylglutaryl-CoA Reductase. *J. Biol. Chem.* **2003**, *278*, 19933–19938.
- (12) Bischoff, K.; Rodwell, V. 3-Hydroxy-3-methylglutaryl-coenzyme A reductase from *Haloferax volcanii*: purification, characterization, and expression in *Escherichia coli*. *J. Bacteriol.* **1996**, *178*, 19–23.
- (13) Kim, D.-Y.; Stauffacher, C. V.; Rodwell, V. W. Dual coenzyme specificity of *Archaeoglobus fulgidus* HMG-CoA reductase. *Protein Sci.* **2000**, *9*, 1226–1234.
- (14) Alberts, A. W.; Chen, J.; Kuron, G.; Hunt, V.; Huff, J.; Hoffman, C.; Rothrock, J.; Lopez, M.; Joshua, H.; Harris, E.; Patchett, A.; Monaghan, R.; Currie, S.; Stapley, E.; Albers-Schonberg, G.; Hensens, O.; Hirshfield, J.; Hoogsteen, K.; Liesch, J.; Springer, J. Mevinolin: a highly potent competitive inhibitor of hydroxymethylglutaryl-coenzyme A reductase and a cholesterol-lowering agent. *Proc. Natl. Acad. Sci. USA* **1980**, *77*, 3957–3961.
- (15) Arguelles, N.; Sanchez-Sandoval, E.; Mendieta, A.; Villa-Tanaca, L.; Garduno-Siciliano, L.; Jimenez, F.; Cruz, M. D.; Medina-Franco, J. L.; Chamorro-Cevallos, G.; Tamariz, J. Design, synthesis, and docking of highly hypolipidemic agents: *Schizosaccharomyces pombe* as a new

- model for evaluating alpha-asarone-based HMG-CoA reductase inhibitors. *Bioorg. Med. Chem.* **2010**, *18*, 4238–4248.
- (16) Zhang, Q. Y.; Wan, J.; Xu, X.; Yang, G. F.; Ren, Y. L.; Liu, J. J.; Wang, H.; Guo, Y. Structure-Based Rational Quest for Potential Novel Inhibitors of Human HMG-CoA Reductase by Combining CoMFA 3D QSAR Modeling and Virtual Screening. *J. Comb. Chem.* **2006**, *9*, 131–138.
- (17) Singh, N.; Tamariz, J.; Chamorro, G.; Medina-Franco, J. L. Inhibitors of HMG-CoA Reductase: Current and Future Prospects. *Mini-Rev. Med. Chem.* **2009**, *9*, 1272–1283.
- (18) Istvan, E. S.; Deisenhofer, J. Structural Mechanism for Statin Inhibition of HMG-CoA Reductase. *Science* **2001**, *292*, 1160–1164.
- (19) Istvan, E. S.; Palnitkar, M.; Buchanan, S. K.; Deisenhofer, J. Crystal structure of the catalytic portion of human HMG-CoA reductase: insights into regulation of activity and catalysis. *Embo J.* **2000**, *19*, 819–830.
- (20) Feng, L.; Zhou, L.; Sun, Y.; Gui, J.; Wang, X.; Wu, P.; Wan, J.; Ren, Y.; Qiu, S.; Wei, X.; Li, J. Specific inhibitions of annonaceous acetogenins on class II 3-hydroxy-3-methylglutaryl coenzyme A reductase from *Streptococcus pneumoniae*. *Bioorg. Med. Chem.* **2011**, *19*, 3512–3519.
- (21) Lawrence, C.; Rodwell, V.; Stauffacher, C. Crystal structure of *Pseudomonas mevalonii* HMG-CoA reductase at 3.0 angstrom resolution. *Science* **1995**, *268*, 1758–1762.
- (22) Tabernero, L.; Bochar, D. A.; Rodwell, V. W.; Stauffacher, C. V. Substrate-induced closure of the flap domain in the ternary complex structures provides insights into the mechanism of catalysis by 3-hydroxy-3-methylglutaryl-CoA reductase. *Proc. Natl. Acad. Sci. USA* **1999**, *96*, 7167–7171.
- (23) Zhang, L. P.; Feng, L. L.; Zhou, L.; Gui, J.; Wan, J. A.; Hu, X. P. Purification, crystallization and preliminary X-ray analysis of 3-hydroxy-3-methylglutaryl-coenzyme A reductase of *Streptococcus pneumoniae*. *Acta Crystallogr. F.* **2010**, *66*, 1500–1502.
- (24) Schwede, T.; Kopp, J.; Guex, N.; Peitsch, M. C. SWISS-MODEL: an automated protein homology-modeling server. *Nucleic Acids Res.* **2003**, *31*, 3381–3385.
- (25) SPECs provides chemistry and chemistry related services that are required in drug discovery. 1987; <http://www.specs.net> (accessed Dec 5, 2011)
- (26) Zhang, Q. Y.; Li, D.; Wei, P.; Zhang, J.; Wan, J.; Ren, Y. L.; Chen, Z. G.; Liu, D. L.; Yu, Z. N.; Feng, L. L. Structure-Based Rational Screening of Novel Hit Compounds with Structural Diversity for Cytochrome P450 Sterol 14 alpha-Demethylase from *Penicillium digitatum*. *J. Chem. Inf. Model.* **2010**, *50*, 317–325.
- (27) Sarver, R. W.; Bills, E.; Bolton, G.; Bratton, L. D.; Caspers, N. L.; Dunbar, J. B.; Harris, M. S.; Hutchings, R. H.; Kennedy, R. M.; Larsen, S. D.; Pavlovsky, A.; Pfefferkorn, J. A.; Bainbridge, G. Thermodynamic and Structure Guided Design of Statin Based Inhibitors of 3-Hydroxy-3-Methylglutaryl Coenzyme A Reductase. *J. Med. Chem.* **2008**, *51*, 3804–3813.
- (28) Case, D. A.; Darden, T. A.; Cheatham, T. E.; Simmerling, C. L.; Wang, J.; Duke, R. E.; Luo, R.; Merz, K. M.; Wang, B.; Pearlman, D. A.; Crowley, M.; Brozell, S.; Tsui, V.; Gohlke, H.; Mongan, J.; Hornak, V.; Cui, G.; Beroza, P.; Schafmeister, C.; Caldwell, J. W.; Ross, W. S.; Kollman, P. A. AMBER, version 8; University of California: San Francisco, CA, 2004.
- (29) Morris, A. L.; MacArthur, M. W.; Hutchinson, E. G.; Thornton, J. M. Stereochemical quality of protein structure coordinates. *Proteins: Structure, Function, Bioinformatics* **1992**, *12*, 345–364.
- (30) Sybyl 7.3; Tripos Inc.: St. Louis, MO, 2003; <http://www.tripos.com> (accessed Dec 5, 2011).
- (31) Istvan, E. S. Bacterial and mammalian HMG-CoA reductases: related enzymes with distinct architectures. *Curr. Opin. Struc. Biol.* **2001**, *11*, 746–751.
- (32) Frimpong, K.; Rodwell, V. W. Catalysis by Syrian hamster 3-hydroxy-3-methylglutaryl-coenzyme A reductase. Proposed roles of histidine 865, glutamate 558, and aspartate 766. *J. Biol. Chem.* **1994**, *269*, 11478–11483.
- (33) Wang, Y.; Darnay, B. G.; Rodwell, V. W. Identification of the principal catalytically important acidic residue of 3-hydroxy-3-methylglutaryl coenzyme A reductase. *J. Biol. Chem.* **1990**, *265*, 21634–21641.
- (34) Darnay, B. G.; Wang, Y.; Rodwell, V. W. Identification of the catalytically important histidine of 3-hydroxy-3-methylglutaryl-coenzyme A reductase. *J. Biol. Chem.* **1992**, *267*, 15064–15070.
- (35) Tempel, W.; Rabeh, W. M.; Bogan, K. L.; Belenky, P.; Wojcik, M.; Seidle, H. F.; Nedylkova, L.; Yang, T.; Sauve, A. A.; Park, H. -W.; Brenner, C. Nicotinamide Riboside Kinase Structures Reveal New Pathways to NAD. *PLoS Biol.* **2007**, *5*, e263–e263.
- (36) Rusinko, I. A.; Skell, J. M.; Balducci, R.; McGarity, C. M.; Pearlman, R. S. Concord, A Program for the Rapid Generation of High Quality Approximate 3-Dimensional Molecular Structures. The University of Texas at Austin and Tripos Associates: St. Louis, MO. 1988.
- (37) Pearlman, R. S. Rapid Generation of High Quality Approximate 3D Molecular Structures. *Chem. Des. Aut. News* **1987**, *2*, 1–6.
- (38) Wang, J. M.; Wang, W.; Kollman, P. A. Antechamber: An accessory software package for molecular mechanical calculations. *Abstr. Am. Chem. Soc.* **2001**, *222*, U403–U403.
- (39) Jain, A. N. Scoring noncovalent protein-ligand interactions: A continuous differentiable function tuned to compute binding affinities. *J. Comput. Aid. Mol. Des.* **1996**, *10*, 427–440.
- (40) Ding, F.; Huang, J.; Lin, J.; Li, Z.; Liu, F.; Jiang, Z.; Sun, Y. A study of the binding of C.I. Mordant Red 3 with bovine serum albumin using fluorescence spectroscopy. *Dyes. Pigments* **2009**, *82*, 65–70.
- (41) Llano-Sotelo, B.; Chow, C. S. RNA-aminoglycoside antibiotic interactions: Fluorescence detection of binding and conformational change. *Bioorg. Med. Chem. Lett.* **1999**, *9*, 213–216.
- (42) Ahmad, B.; Parveen, S.; Khan, R. H. Effect of Albumin Conformation on the Binding of Ciprofloxacin to Human Serum Albumin: A Novel Approach Directly Assigning Binding Site. *Biomacromolecules* **2006**, *7*, 1350–1356.